

Delft University of Technology

ET4173

INTRODUCTION TO UWB TECHNOLOGY, SYSTEMS AND APPLICATIONS

Clutter Suppression for Detection and Positioning with Multiple IR-UWB Radars

Final assignment | Project - 12

Authors:

Yanqi Hong (5884683) Y.Hong-8@student.tudelft.nl

June 18, 2024



Abstract

This report analyzes various clutter suppression (CS) techniques for human tracking in Impulse Radio Ultra-Wideband (IR-UWB) radar systems. Clutter from environmental reflections, multipath effects, and noise degrades system performance. We evaluate adaptive clutter suppression, the Constant False Alarm Rate (CFAR) detector, and decentralized tracking using a particle filter (PF). Using a four-radar setup to track a person on a triangular path in a cluttered environment, results show that CS techniques significantly enhance accuracy. The CFAR detector, especially when decentralized, achieves the lowest false alarm rate (0.5326) and mean distance error (0.2448 m) compared to the baseline without CS. Decentralized tracking improves performance with lower false alarm rates, though with slightly increased processing delays. This study highlights the crucial role of CS techniques in improving IR-UWB radar reliability and accuracy for human tracking in cluttered settings. Besides, the choice of the CS method depends on balancing accuracy, processing time, and implementation complexity.

1 Introduction

Impulse Radio Ultra-Wideband (IR-UWB) radar technology has emerged as a potent tool for indoor sensing applications due to its high temporal resolution, penetration capability, and low power consumption. These attributes make IR-UWB radars highly suitable for tasks such as object detection and positioning in complex environments. However, the efficacy of these applications is often hampered by high false alarm rates, commonly referred to as clutter. Clutter in radar systems can arise from a multitude of sources, including environmental reflections, multipath effects, and inherent noise, leading to significant challenges in accurately detecting and positioning objects.

In the context of object tracking with multiple IR-UWB radars, the clutter can cause the false alarm issue which can be obvious in three primary forms: when there are no targets and local false alarms are associated, when a single target is present and local false alarms mix with true measurements, and when multiple targets are present and measurements are incorrectly associated between them [1]. The presence of such false alarms can severely degrade the performance of detection and positioning systems, resulting in increased false alarms and reduced precision in target localization. Therefore, effective clutter suppression techniques are crucial to enhance the reliability and accuracy of IR-UWB radar systems.

In this project, we aim to localize and track a person using four IR-UWB radars, employing various approaches and comparing the false alarm rates of these methods. In Chapter 2, we will describe the original data. Chapters 3 through 7 will cover the technical details of the methodologies used. Finally, in Chapter 8, we will compare the tracking results with and without clutter suppression methods.

2 Radar Data Overview

In this project, we utilize four PulsOn 410 radio transceivers for human tracking. These radar sensors are part of a monostatic radar platform known for their compactness, cost-effectiveness, and substantial RF bandwidth centered around 4 GHz [2]. The system comprises four radar units: UWB 101, UWB 102, UWB 104, and UWB 106, each positioned as indicated in Figure 1.

In the environment is a chair equipped with a metal plate, located at Point G in Figure 1. This setup plays a crucial role in calibrating and testing the radar's performance in cluttered environments. A man follows a triangular path defined by the points I-C-A in Figure 1, representing the true trajectory of interest in this study. Figure 2 shows the real measurement for human localization.

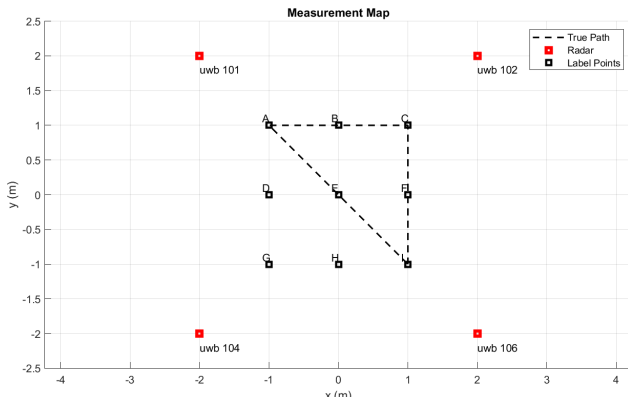


Figure 1: UWB Radar Measurement Environment Map

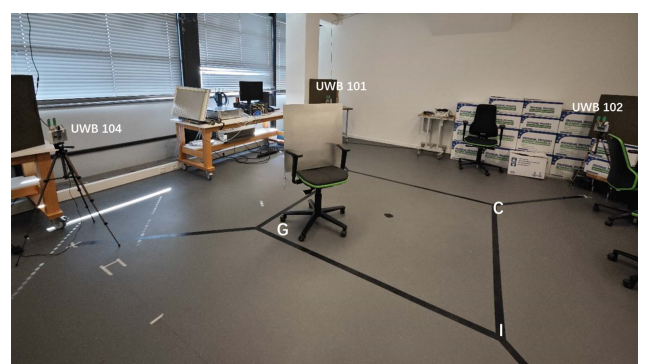


Figure 2: Measurement environment

The data acquisition process operates with a sample time of 0.0612 seconds, utilizing a fast time bin number of 480 and a slow time bin number of 1024 for detailed analysis of reflected signals. The range plot is depicted in Figure 3. Observing the plot, it becomes evident that the raw data shows numerous horizontal stripes in the time-range representation, primarily due to clutter and environmental noise. UWB 104 is notably affected by clutter, particularly because of its proximity to the metal plate. This extraneous information has the potential to obscure the desired signal and increase the false alarm rate. Considering the actual human walking interval, we will select the bins from slow time 55 to 760 in the range-time plot for the following processing. Therefore, it is imperative to implement robust clutter suppression (CS) techniques, which will be discussed in Chapter 3.

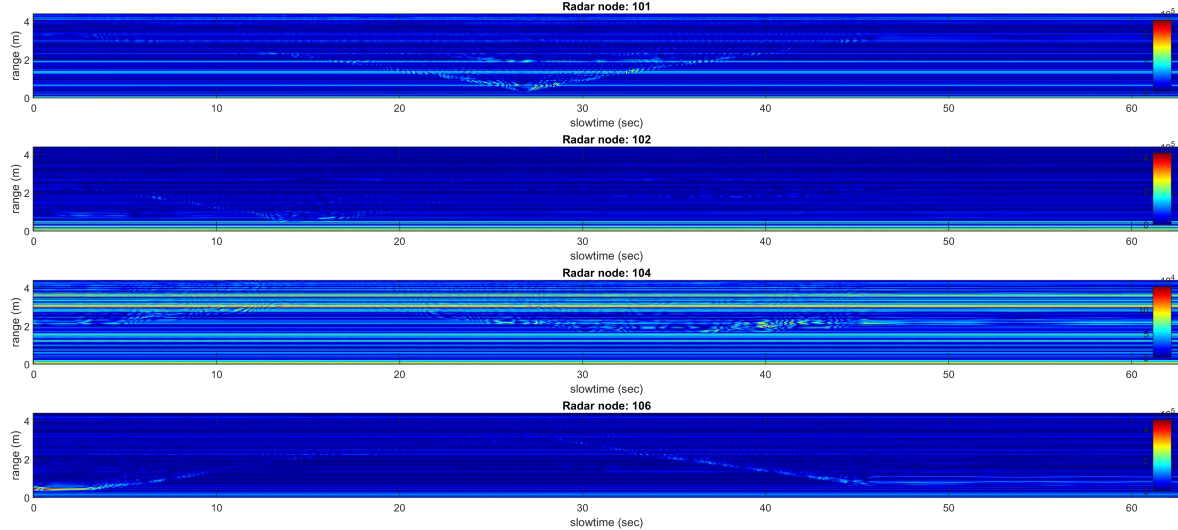


Figure 3: Received original Range-Time plot for four UWB radars

3 Adaptive Clutter Suppression

To eliminate the influence of clutter, an adaptive clutter algorithm based on the method shown in [3] is used. This process of adaptive clutter suppression can be represented by Equation 1 [3]. In Equation 1, k denotes the index of the slow time bin, $r(t)$ is the received signal, $c(t)$ is the clutter noise, and $y(t)$ is the processed signal. $\tilde{r}_k(t)$ and $\tilde{y}_k(t)$ represent the normalized envelopes of $r_k(t)$ and $y_k(t)$, respectively. The envelope is obtained from the Hilbert Transform of $r_k(t)$ and $y_k(t)$. The application ratio $a_k(t)$ is updated based on the value of the envelope.

A high application ratio improves SNR but delays accurate clutter signal capture, risking inaccurate target movement representation. Conversely, a low application ratio quickly extracts moving targets but suppresses both clutter and target signals, potentially leading to insufficient SNR and missed detections [3]. The variable $d_k(t)$ is used to determine the application ratio for the next scan, using the envelope of two signals. If there is motion at a certain distance t_0 , $\tilde{y}_k(t_0)$ would be greater than $\tilde{r}_k(t_0)$ at that point. Therefore, $d_k(t_0)$ would be one and $a_k(t_0)$ would have the value a_{\max} to maximize SNR. Conversely, $d_k(t)$ has a lower application ratio according to the ratio of $\tilde{r}_k(t)$ and $\tilde{y}_k(t)$ at points with little or temporary motion [3]. By using this method, $a_k(t)$ can be adjusted based on different circumstances. During the iterative period, some slow-time bins may contain all zeros due to measurement errors. In these zero slow time bins, the adaptive CS method is skipped, and the value in the zero slow time bins is set equal to the last slow time bin with a valid value.

By selecting $a_{\max} = 0.6$ and $a_{\min} = 0.2$ and applying the adaptive CS method along with normalization, the filtered data is presented in Figure 4. It is evident that the horizontal stripes, indicative of clutter and noise, have been significantly reduced in Figure 4 compared with Figure 3.

$$\begin{aligned}
 y_k(t) &= r_k(t) - c_k(t) \\
 d_k(t) &= \frac{\min(\tilde{r}_k(t), \tilde{y}_k(t))}{\tilde{r}_k(t)} \\
 a_k(t) &= a_{\min} + (a_{\max} - a_{\min}) d_k(t) \\
 c_{k+1}(t) &= a_k(t)c_k(t) + (1 - a_k(t))r_k(t)
 \end{aligned} \tag{1}$$

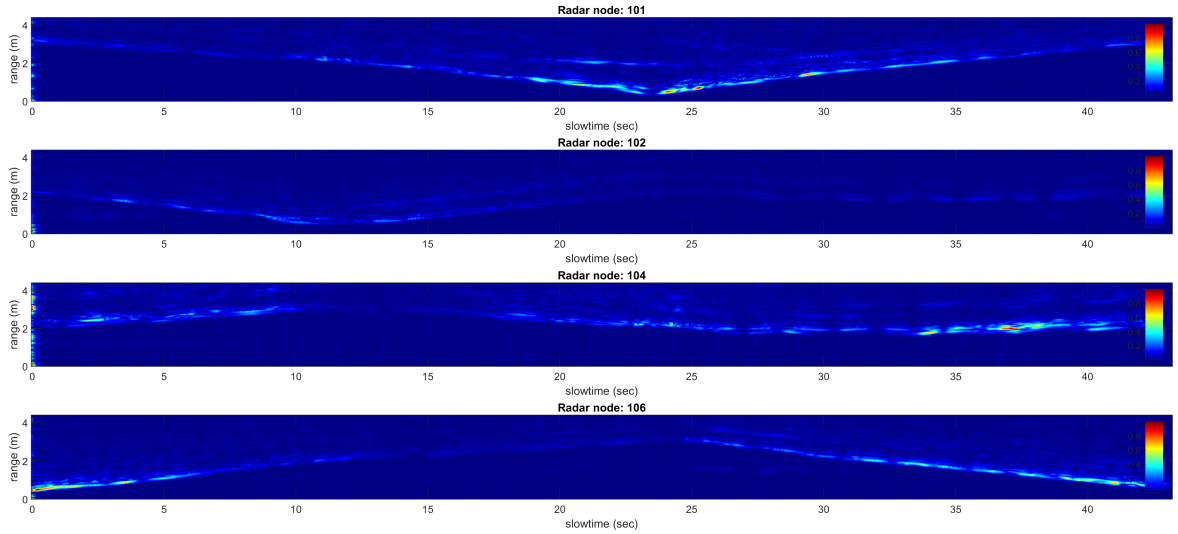


Figure 4: Range Time Plot after adaptive CS process

4 Detector

From Figure 4, it is evident that the light blue area indicates the position where the radar signal is reflected, representing the range of the human presence relative to the radar. To determine the estimated range, we will use two methods: The first method employs a static threshold to detect the estimated range, known as the Neyman-Pearson (NP) detector. The second method uses a Constant False Alarm Rate (CFAR) detector, an adaptive approach that detects the target signal amidst background noise while maintaining a constant probability of false detection.

4.1 NP Detector

In the NP Detector, the core concept is to establish a threshold that can distinguish between the estimated range and the non-estimated range. For this project, we selected a threshold of 0.035. However, exclusive reliance on this threshold for target signal detection can lead to a proliferation of false alarms and significant fluctuations in the estimated range curve, attributable to clutter or noise interference. This phenomenon is evident in the detection results (estimated range curve), where the red line in the first plot of Figure 5 illustrates these false detection points in UWB 102.

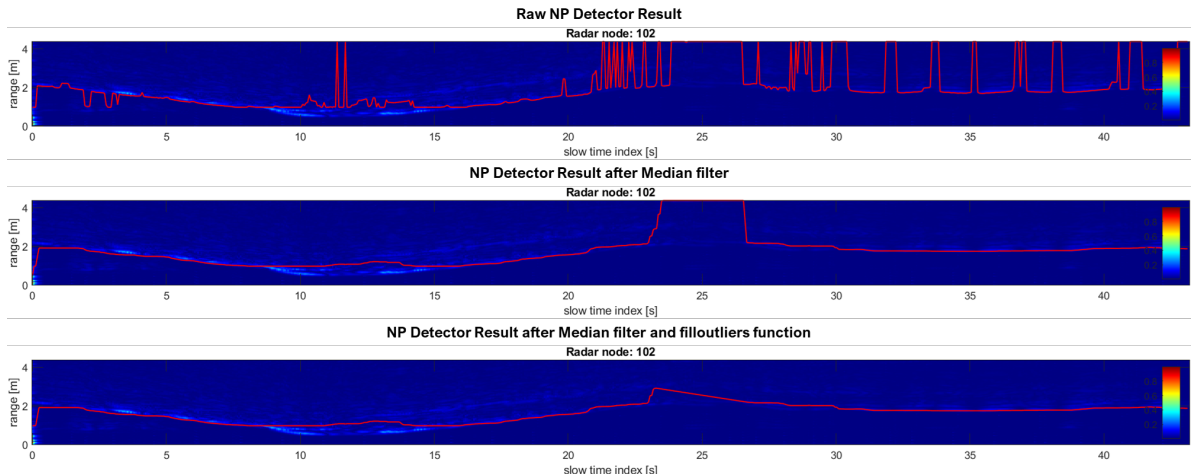


Figure 5: Comparison between the raw NP detector result and the detection result after post-process in UWB 102

To mitigate the influence of clutter, we employed two post-processing methods: a median filter and the `filloutliers` function in MATLAB. These methods smooth the estimated range curve and interpolate outlier values. The outcomes of comparing these post-processing techniques and the raw NP detector result are shown in Figure 5, where it is evident that false alarms caused by clutter and fluctuations induced by noise are significantly reduced.

4.2 CFAR Detector

The CFAR detector is essential for detecting targets within cluttered environments. The Cell Averaging CFAR (CACFAR) is a variant of CFAR that is particularly adept at handling heterogeneous background noise. It operates by comparing the signal level of a "cell" or pixel, against the average level of surrounding cells within a defined "training band". The Guard Band is a set of cells immediately adjacent to the cell under test that is excluded from this averaging process to prevent the target from skewing the noise estimate.

In this project, we utilize the `CFARDetector2D` function in MATLAB to implement CACFAR for localizing targets across multiple radar nodes. The parameters for the Guard Band and Training Band sizes are set to [10, 15] and [36, 54] respectively, reflecting the target signal's proportion of 2 : 3 (*fast time bin : slow time bin* = 480 : 705 \approx 2 : 3). This configuration is optimized to maintain a false alarm rate at 0.156, which is achieved through careful tuning to get the best detection result.

The CFAR process in this project unfolds in several steps which is also shown in Figure 6:

1. **Boundary Calculation:** The detection threshold is established by calculating the noise level within the training band in the boundary of detection.
2. **CACFAR Detection:** The actual detection of targets is performed, where each cell's signal is compared against the threshold. Based on the CACFAR detection, we can get the detection mask indicating which point is judged to be the target.
3. **Post-Processing:** The raw detection matrix is converted into a range plot, and further improved through various techniques.

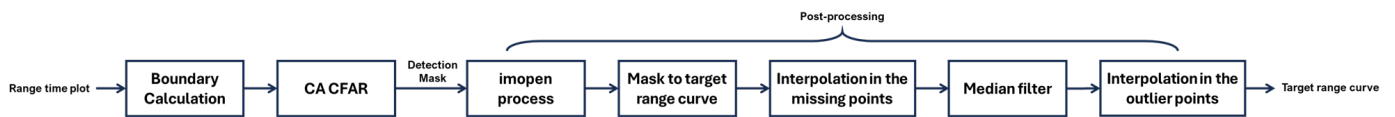


Figure 6: CFAR workflow

According to the Boundary Calculation, to address the challenge of detecting targets at the edge of the signal range, where the boundary may be smaller than the signal size. We extend the radar range time plot by replicating the outermost 80 indices from each edge to the opposite side, thus enlarging the effective detection area and ensuring edge targets are not missed. Once we get the suitable boundary, we can use the `CFARDetector2D` function to achieve the raw detection mask which is shown in the left plot in the Figure 7. The yellow points in Figure 7 denote the target points.

According to Post-processing, three key processes will be discussed detailed:

- **Morphological Opening:** Morphological opening is an image processing operation that involves eroding an image followed by dilation, used primarily to remove small objects and noise while preserving the shape and size of larger structures. Because we can seem the matrix as a kind of image, so we can use morphological opening to eliminate the scatter points in the matrix. Using MATLAB's `imopen` function with a structuring element defined by `strel('square', 12)`, we perform morphological opening to remove isolated scatter points (error detection points), thereby clarifying the detection mask and reducing false alarms before we convert the detection mask into the estimated range. In Figure 7, it is clear to find that after the `imopen` process, the amount of scatter points (especially in the bottom part of the plot) disappear.
- **Interpolation:** To ensure continuity in the estimated range, interpolation is applied at points where the target may have been missed. For example, in the red circle of the right part of Figure 7, there exists missing detection points which are necessary to interpolate after we convert the detection mask into the estimated range curve. Additionally, similar to the post-processing in the NP detector, the `filloutliers` function is also used to identify and interpolate outlier values, further mitigating false alarms.
- **Median Filtering:** In the end, a median filter is applied to smooth the estimated range curve, enhancing the overall clarity and reliability of the target localization.

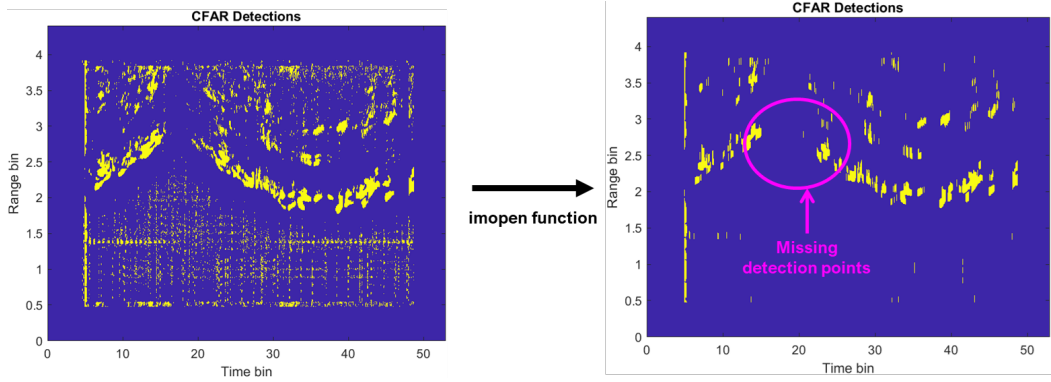


Figure 7: Comparison of raw CFAR detection mask and the mask after imopen process for UWB 104

This comprehensive approach to CFAR processing not only enhances target detection accuracy but also minimizes the probability of false alarms, ensuring more precise localization results. Figure 8 shows the estimated range of the CFAR detector denoted as the red line.

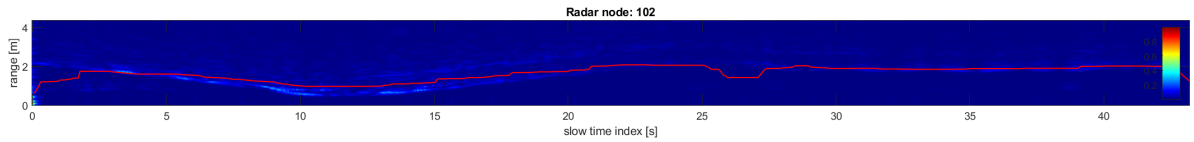


Figure 8: CFAR estimated range curve of UWB 102

5 Decentralized Tracking

After establishing the estimated range curve, the application of a 1D tracking method is proposed for each radar node to track the curve independently. This method effectively diminishes the influence of clutter and further decreases the false alarm rate. Such a technique, involving the 1D tracking by individual radar nodes before the integration of their data for localization, is termed decentralized tracking. It enhances the precision of the target localization by filtering out noise and discrepancies inherent in the radar signals. Conversely, the centralized tracking method bypasses this individual node processing, directly utilizing the estimated range from each radar node for localization.

Algorithm 1 Particle Filter for 1D Position Estimation

Input: InputPosition: Vector of observed positions (estimated range curve),
numParticles: Number of particles,
windowSize: Size of observation buffer window

Output: FilteredPosition: Vector of filtered positions

1 Initialization:

- 2 1. Initialize the particle filter ("stateEstimatorPF")
2. Set up the observation buffer and vectors for predicted and corrected positions.

3 Main Loop

- 4 **for** $i \leftarrow 1$ **to** $\text{length}(\text{InputPosition})$ **do**
 - 5 1. Update the observation buffer with the current input position:
 $\text{Buffer}[\text{mod}(i - 1, \text{windowSize}) + 1] \leftarrow \text{InputPosition}[i]$
 - 5 2. Predict the current state using the particle filter:
 $[\text{PosPred}[i], \text{PosCov}] \leftarrow \text{Particle Filter Prediction}$
 - 5 3. Correct the state estimate using observations from the buffer:
for $k \leftarrow 1$ **to** windowSize **do**
 - 6 4. Skip unfilled buffer entries
 - 6 5. Corrects the measurement, state, and state estimation error covariance:
 $[\text{PosCorrected}[i], \text{PosCov}] \leftarrow \text{correct}(\text{pf}, \text{currentObservation})$

- 7 6. Return the vector of corrected positions as the filtered position output.

Return

- 8 $\text{FilteredPosition} \leftarrow \text{PosCorrected}$
-

In this project, a 1D particle filter (PF) is employed as the tracking method for decentralized tracking. The particle filter is a sequential Monte Carlo method that approximates the posterior probability density function (PDF) of a system's state by a set of weighted samples. These samples, also known as particles, evolve over time to incorporate new measurements. The MATLAB function `stateEstimatorPF` is used to implement the PF. In this project, we set the number of particles for 1D tracking to 350.

However, noise and clutter can significantly degrade the accuracy of individual observations in the PF. To address this issue, a buffer window of configurable size is employed. This buffer window integrates observations over a defined time horizon, effectively smoothing the estimated position. This averaging process reduces the impact of noise and clutter, leading to a more accurate representation of the system's true state and a decrease in the false alarm rate further. The general algorithm of the buffer window process is shown in Algorithm 1. In this project, the buffer window size is set to 35.

Figure 9 shows the estimated range curve after PF for the NP detector and CFAR detector in UWB 102. Compared with the estimated range curve without PF (centralized tracking) in Figure 5 and Figure 8, the curve with PF is smoother and closer to the real range curve.

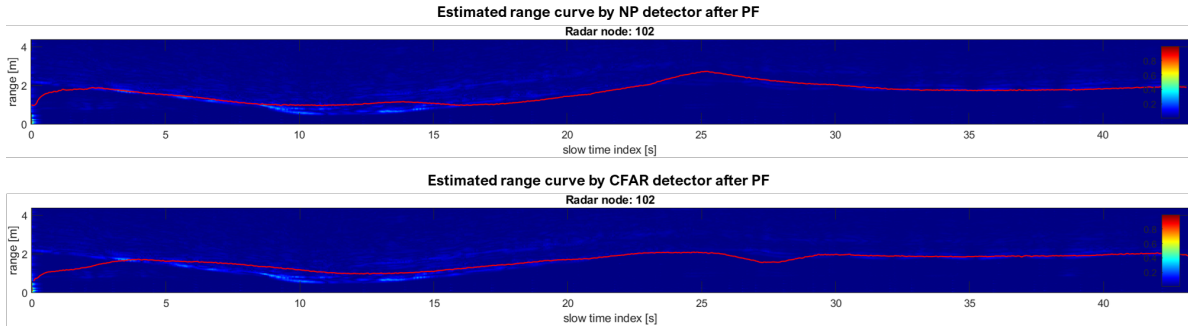


Figure 9: Estimated range curve after PF in UWB 102

6 Localization

By utilizing the estimated range from four radars, we can employ the Least Squares Error (LSE) method to estimate the position of the human. The equation for the LSE is depicted in Equation 2, where \mathbf{x} , \mathbf{h} , and θ are defined in Equation 3. In Equation 3, r_1 to r_4 represent the estimated ranges from four radars respectively, while x_1 to x_4 and y_1 to y_4 denote the coordinates of the four radars. P_x and P_y denote the estimated position of the human. Therefore, the estimated human position can be obtained using Equation 4.

$$\min_{\theta} \|\mathbf{x} - \mathbf{h}\theta\|_2^2 \quad (2)$$

$$\begin{aligned} \mathbf{x} &= \begin{bmatrix} r_1^2 - r_4^2 - x_1^2 + x_4^2 - y_1^2 + y_4^2 \\ r_2^2 - r_4^2 - x_2^2 + x_4^2 - y_2^2 + y_4^2 \\ r_3^2 - r_4^2 - x_3^2 + x_4^2 - y_3^2 + y_4^2 \end{bmatrix} \\ \mathbf{h} &= 2 \begin{bmatrix} x_4 - x_1 & y_4 - y_1 \\ x_4 - x_2 & y_4 - y_2 \\ x_4 - x_3 & y_4 - y_3 \end{bmatrix} \\ \theta &= \begin{bmatrix} P_x \\ P_y \end{bmatrix} \end{aligned} \quad (3)$$

$$\theta = (\mathbf{h}^\top \mathbf{h})^{-1} \mathbf{h}^\top \mathbf{x} \quad (4)$$

The localization results of the NP detector after decentralized tracking are depicted in Figure 10. The blue dots in the figure represent the estimated positions of the human. The green area indicates the actual human walking region, considering an average shoulder width of 37 cm. From the green area, it is very easy to find out which points are not in the region of the walking path of the human. According to the localization point in Figure 10, it can be obvious that the estimated positions can generally reflect the actual walking path.

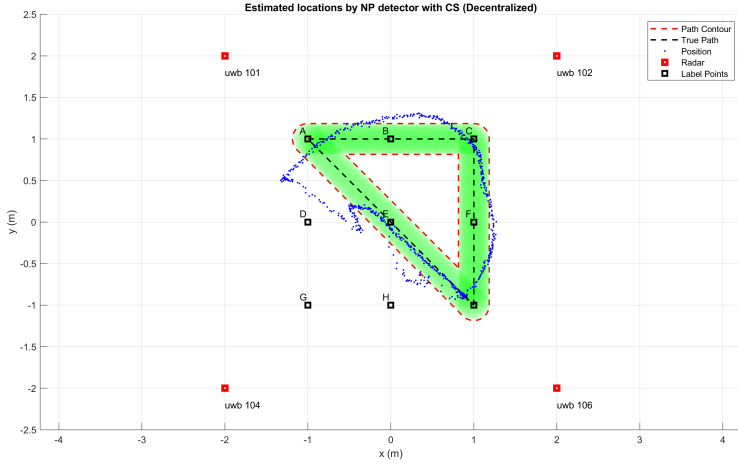


Figure 10: Estimated locations by NP detector (Decentralized)

7 2D Tracking

Based on the estimated position, we can use 2D tracking to estimate the human walking trajectory. The 2D Particle Filter (2D PF) is utilized for estimating human walking trajectories, building upon the principles of the 1D PF detailed in Chapter 5. It features two tunable parameters: 10,000 particles for state space sampling and a buffer window size of 50 to balance tracking responsiveness against noise.

The 2D PF tracking results for NP and CFAR detectors, encompassing both centralized and decentralized tracking, are illustrated in Figure 11. The red line in the plot represents the estimated trajectory. It is evident that the 2D PF effectively tracks the primary position points and mitigates some of the error in estimation, providing a clearer depiction of the actual path taken by the human.

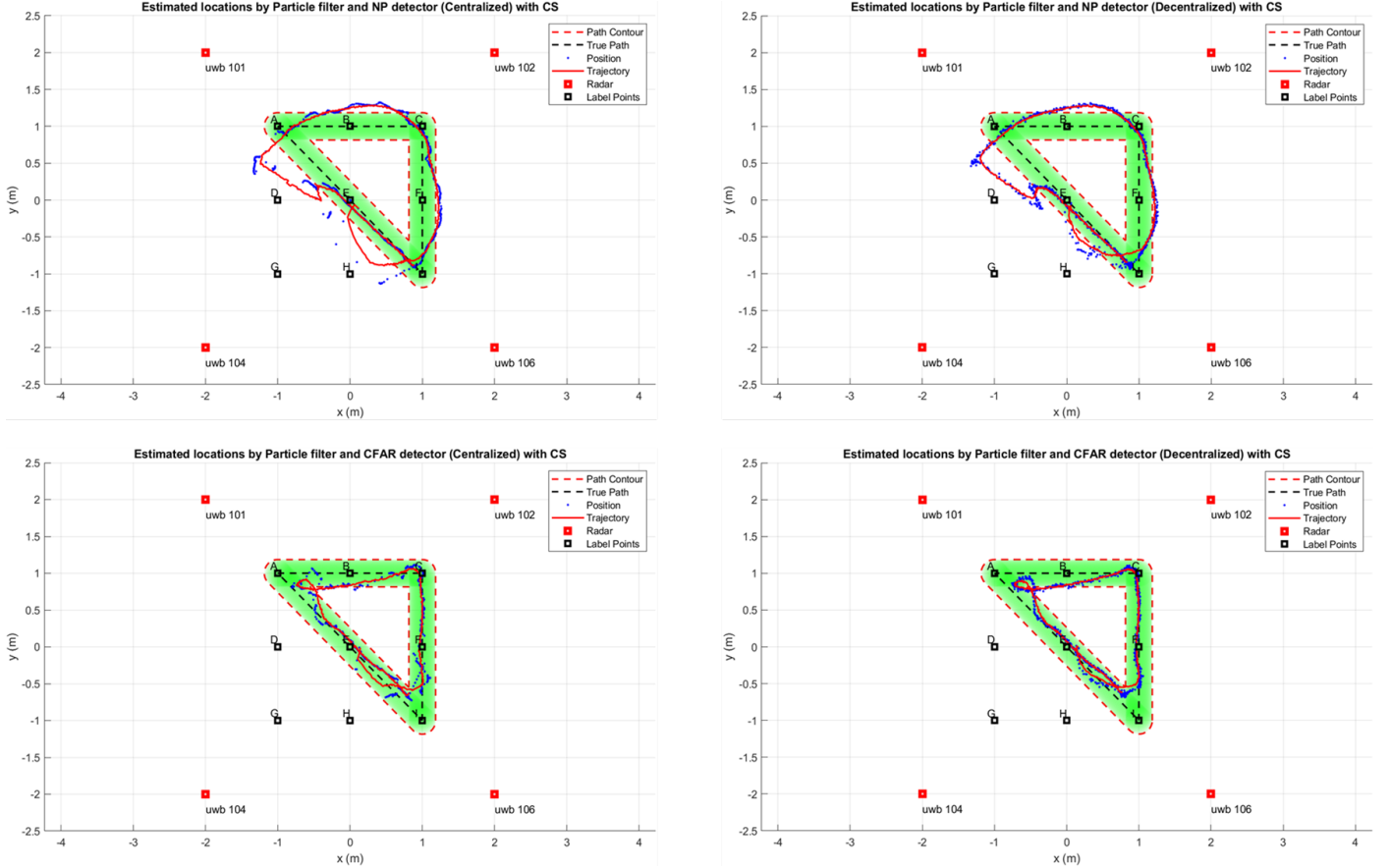


Figure 11: PF tracking trajectory result of NP and CFAR detector

8 Evaluation

To assess the performance of the localization system using various methods, the primary evaluation metrics are the false alarm rate and the mean distance error. Additionally, this chapter evaluates the system's performance with and without clutter suppression (CS) techniques, such as Adaptive Clutter Suppression, Morphological Opening, decentralized tracking, and interpolation for handling outlier values. The localization system without CS is called the baseline in this project.

8.1 Evaluation metric

The false alarm rate measures how frequently a system indicates an event or condition that has not actually occurred. To calculate the false alarm rate, we assume the human is walking at a constant speed. Under this assumption, we establish the actual position of the human at every moment. Next, we compute the distance between the estimated trajectory point by 2D PF and the actual point. If this distance is less than 0.185 meters (half of the human shoulder width, which is 0.37 meters), the estimated trajectory point is considered a correct detection. Conversely, if the distance exceeds 0.185 meters, it is classified as a false alarm. The false alarm rate is then determined by calculating the proportion of false alarm points among all detected points. Besides, to access the system further, the mean distance error between every estimated trajectory point and the actual points is also served as another evaluation metric.

8.2 Baseline

By skipping every CS technique including Adaptive Clutter Suppression, Morphological Opening, decentralized tracking, and interpolation for handling outlier values, we can get the estimated location and trajectory by NP and CFAR showing in Figure 12. Both position results in Figure 12 can not represent the actual movement. The reason is that the clutter is so strong that both the NP and CFAR detector cannot find out where is the target range shown in Figure 13.

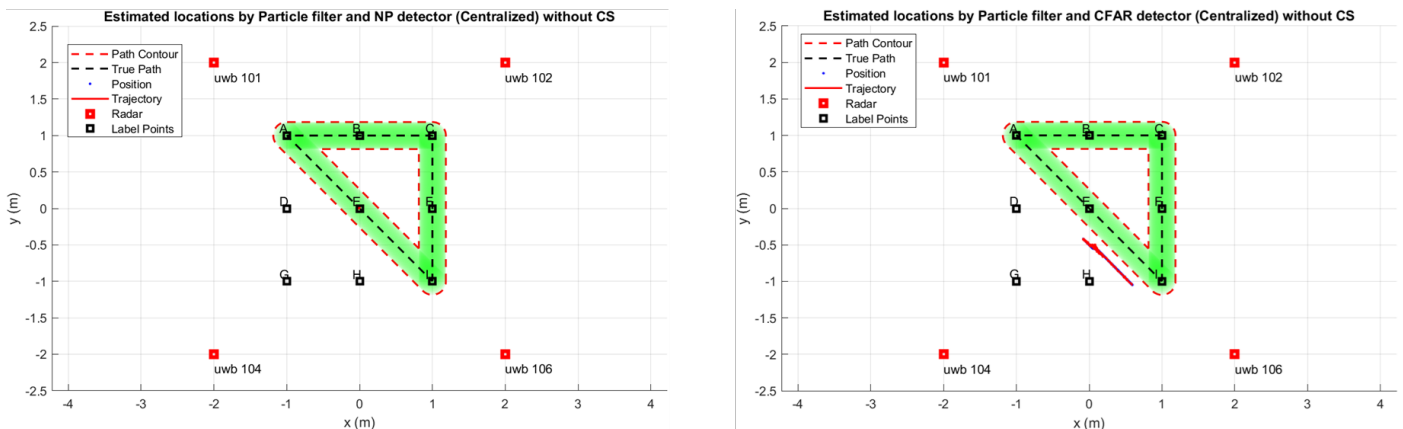


Figure 12: Localization and tracking result without CS technique

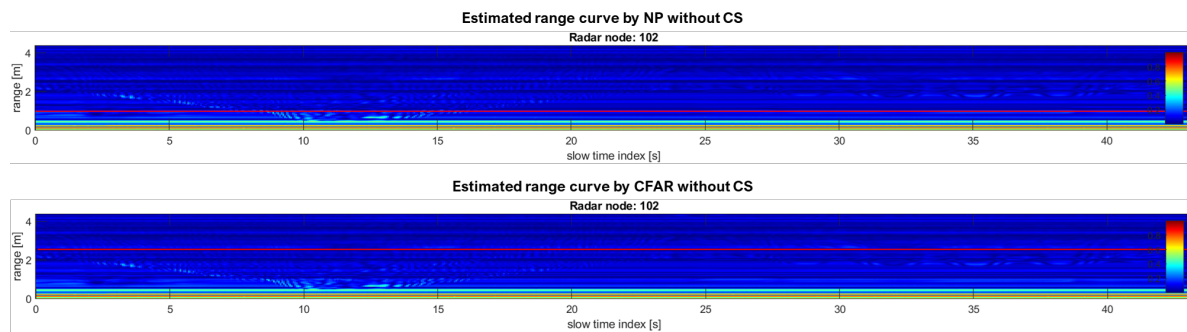


Figure 13: Estimated range by NP and CFAR detector without CS techniques

8.3 Comparison and Discussion

Based on the evaluation metric, the false alarm rate and mean distance error of baseline and the localization with CS are listed in Table 1. When comparing the performance of localization methods with clutter suppression

to the baseline (no clutter suppression), it is evident that clutter suppression significantly enhances the system's accuracy. The False Alarm Rate is obviously reduced in all methods employing CS, with the CFAR decentralized method achieving the lowest rate of 0.5326, compared to the baseline rates of 0.949 and 1 for NP and CFAR centralized methods, respectively. Similarly, the Mean Distance Error is substantially lower with CS, with the CFAR decentralized method again outperforming others at 0.2448 m, in contrast to the baseline errors of 0.9986 m and 1.0852 m.

Further analyzing the performance of different localization methods with CS, the decentralized approaches, both NP and CFAR, demonstrate superior results over their centralized counterparts. The decentralized NP method exhibits a lower False Alarm Rate of 0.5567 compared to 0.6586 for the centralized NP. In terms of Mean Distance Error, the decentralized CFAR method shows a minimal error of 0.2448 m, which is marginally better than the centralized CFAR's 0.2458 m. In conclusion, the implementation of clutter suppression in radar signal localization methods significantly improves the system's performance, with decentralized methods showing a slight edge over centralized ones.

When assessing the NP and CFAR detectors, the centralized CFAR method registers a marginally elevated False Alarm Rate at 0.6643 versus the NP's 0.6586. However, it compensates with a reduced Mean Distance Error of 0.2458 m, reflecting enhanced precision in pinpointing targets. This trade-off suggests that while the CFAR may occasionally misidentify some points, it generally provides more accurate localization outcomes. Inversely, the decentralized CFAR method not only reduces the False Alarm Rate to 0.5326, outperforming the NP's 0.5567 but also minimizes the Mean Distance Error to 0.2448 m, compared to NP's 0.2774 m. These results underscore the effectiveness of the CFAR method in clutter suppression, offering a more precise and reliable radar signal localization in both centralized and decentralized configurations.

While the decentralized method boasts a lower false alarm rate and reduced mean distance error, it suffers from time delay issues. Utilizing the `finddelay` function in MATLAB, we determined that the delay time for NP detector decentralized tracking compared to centralized tracking is 0.612 s, and for CFAR detector decentralized tracking versus centralized tracking, it is 0.5508 s. These findings demonstrate the importance of selecting the most suitable localization method based on practical requirements. For applications demanding high precision, the decentralized method may be preferable. Conversely, in scenarios where time delay is a critical factor, the centralized approach might be the better option.

Evaluation Method	Localization with CS				Baseline (no CS)	
	NP centralized	NP decentralized	CFAR centralized	CFAR decentralized	NP centralized	CFAR centralized
False Alarm Rate	0.6586	0.5567	0.6643	0.5326	0.949	1
Mean Distance Error (m)	0.2986	0.2774	0.2458	0.2448	0.9986	1.0852

Table 1: Comparison between different localization methods

9 Conclusion

In this project, we assess clutter suppression methods to improve the performance of Impulse Radio Ultra-Wideband (IR-UWB) radar for indoor tracking. Techniques like adaptive suppression, morphological opening, decentralized tracking, and interpolation significantly enhanced performance. Decentralized tracking with Neyman-Pearson and Constant False Alarm Rate (CFAR) detectors was superior, especially the decentralized CFAR, which achieved a false alarm rate of 0.5326 and a mean distance error of 0.2448 m. Despite their efficiency, decentralized methods have time delays, requiring careful selection based on application needs. Future work can focus on implementing some advanced algorithms (such as machine learning-based algorithms) and reducing time delays for real-time use. In conclusion, this project shows the effectiveness of using the clutter suppression method to improve IR-UWB radar accuracy for human tracking indoors.

References

- [1] Chiani, M., Giorgetti, A., & Paolini, E. (2018). Sensor radar for object tracking. *Proceedings of the IEEE*, 106(6), 1022-1041.
- [2] Data Sheet - Time domain. (2018, January 31). studylib.net. <https://studylib.net/doc/18165249/data-sheet-time-domain>
- [3] Yoo, S., Chung, S., Seol, D. M., & Cho, S. H. (2018, September). Adaptive clutter suppression algorithm for detection and positioning using IR-UWB radar. In *2018 9th International Conference on Ultrawideband and Ultrashort Impulse Signals (UWBUSIS)* (pp. 40-43). IEEE.